Ab initio study of the structural, electronic, elastic and magnetic properties of Cu2GdIn, Ag2GdIn and Au2GdIn

ARTICLE *in* PHYSICA B CONDENSED MATTER · SEPTEMBER 2012

Impact Factor: 1.32 · DOI: 10.1016/j.physb.2012.04.012

4 AUTHORS:

Saadi Berri
University of Setif, 19000 Setif, Algeria
16 PUBLICATIONS **46** CITATIONS
SEE PROFILE

D. Maouche
Ferhat Abbas University of Setif
47 PUBLICATIONS **263** CITATIONS
SEE PROFILE

Fares Zerarga
Ferhat Abbas University of Setif
15 PUBLICATIONS **93** CITATIONS
SEE PROFILE

Youcef Medkour
University of Setif 1,Setif, Algeria
26 PUBLICATIONS **74** CITATIONS
SEE PROFILE

Physica B 407 (2012) 3328–3334

Contents lists available at SciVerse ScienceDirect

Physica B

journal homepage: www.elsevier.com/locate/physb

Ab initio study of the structural, electronic, elastic and magnetic properties of Cu_2GdIn, Ag_2GdIn and Au_2GdIn

Saadi Berri [a,*], Djamel Maouche [b], Fares Zerarga [a], Youcef Medkour [a]

[a] Department of Physics, Faculty of sciences, University of Setif, Algeria
[b] Laboratory for Developing New Materials and their Characterizations, University of Setif, Algeria

ARTICLE INFO

Article history:
Received 31 December 2011
Received in revised form
31 March 2012
Accepted 5 April 2012
Available online 10 April 2012

Keywords:
First-principle calculations
Elastic constants
Electronic structure
Magnetic properties

ABSTRACT

We preformed first-principle calculations for the structural, electronic, elastic and magnetic properties of Cu_2GdIn, Ag_2GdIn and Au_2GdIn using the full-potential linearized augmented plane wave (FP-LAPW) scheme within the generalized gradient approximation by Wu and Cohen (GGA-WC), GGA+U, the local spin density approximation (LSDA) and LSDA+U. The lattice parameters, the bulk modulus and its pressure derivative and the elastic constants were determined. Also, we present the band structures and the densities of states. The electronic structures of the ferromagnetic configuration for Heusler compounds (X_2GdIn) have a metallic character. The magnetic moments were mostly contributed by the rare-earth Gd 4f ion.

1. Introduction

Heusler compounds are ternary intermetallic compounds that have the general composition X_2YZ. In this class, X and Y represent d-electron transition metals, and Z denotes an sp-electron element [1]. In recent years, Heusler compounds have been extensively studied, motivated by their gained importance due to advancements in spintronics [2–6]. In contrast to half-metallic ferromagnets (HMFs) [7], only a few Heusler compounds (all of them with a rare earth metal at the Y position) have been successfully implemented as superconductors [8]. Pd_2YSn is the Heusler compound with the highest critical temperature (4.9 K) [9]. The coexistence of antiferromagnetism and superconductivity, demonstrating the manifoldness of the Heusler family, was reported for Pd_2YbSn [10] and Pd_2ErSn [11]. Many of the Heusler compounds have been reported to be HMFs [12,13], and several Co_2-based Heusler compounds have been used as electrodes in magnetic tunnel junctions [14,15]. The hexagonal compound Pd_2CeIn orders antiferromagnetically at 1.23 K [16]. D.B. de Mooij et al. [17] reported that Pt_2GdSn and Pt_2ErSn exhibit ferromagnetic (Tc=20 K) and paramagnetic behavior, respectively. Generally, Heusler compounds (X_2YZ) crystallize in the cubic $L2_1$ structure (space group $Fm\bar{3}m$), in which the lattice consists of interpenetrating fcc sublattices. The crystal structures of these compounds are shown in Fig. 1. Our paper is organized as follows. The theoretical background is presented in Section 2. The results and discussion are presented in Section 3. A summary of our results is given in Section 4.

2. Method of calculations

We have employed first-principles calculations [18,19] using the full-potential linearized augmented plane wave (FP-LAPW) method [20] as implemented in the WIEN2k code [21]. The exchange-correlation effects were described with the parameterization of the generalized gradient approximation (GGA) by Wu and Cohen (GGA-WC) [22], the local spin density approximation (LSDA) [23], GGA+U [24] and LSDA+U [25]. In the calculations reported here, we used the parameter $R_{mt}K_{max}$=9.5 to determine the matrix size (convergence), where K_{max} is the plane wave cut-off and R_{mt} is the smallest atomic sphere radius. We have chosen a muffin-tin (MT) radius of 2.6 a.u. for the Gd and Au atoms. For the In and Ag atoms, the MT radius is 2.5 a.u., and it is 2.4 a.u. for Cu atoms. Within these spheres, the charge density and potential are expanded in terms of the crystal harmonics up to an angular momenta of L=10. A plane wave expansion has been used in the interstitial region. G_{max} was set to 14, where G_{max} is defined as the magnitude of the largest vector in the charge density Fourier expansion. The Monkorst-Pack special k-points were performed using 1500 special k-points in the Brillouin zone for the Cu_2GdIn, Ag_2GdIn and Au_2GdIn compounds [26]. The convergence criteria for the total energy and force were set to 10^{-5} and 10^{-4} eV/Å, respectively. The GGA+U and LSDA+U calculations used an

* Corresponding author. Tel.: +21395115576; fax: +213 36 92 72 10.
E-mail address: berrisaadi12@yahoo.fr (S. Berri).

0921-4526/$ - see front matter © 2012 Elsevier B.V. All rights reserved.
http://dx.doi.org/10.1016/j.physb.2012.04.012

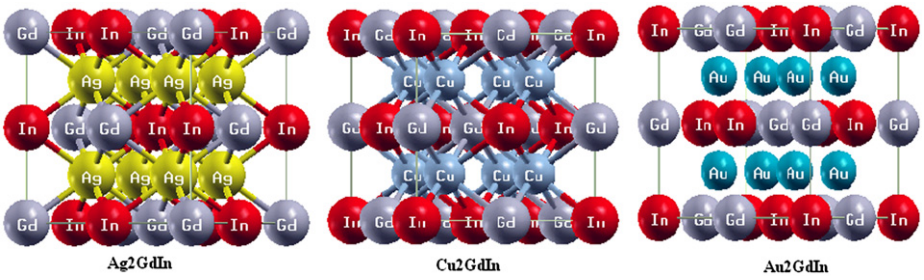

Fig. 1. The crystal structures of Cu_2GdIn, Ag_2GdIn and Au_2GdIn.

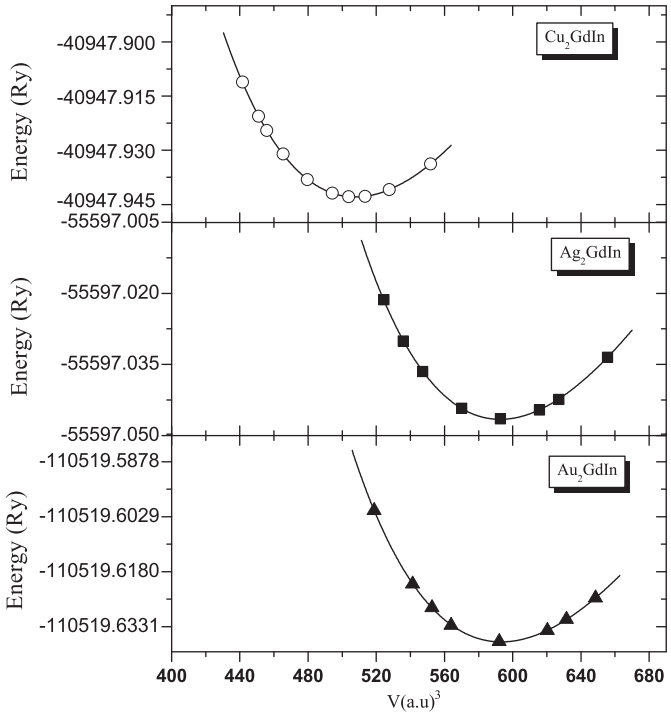

Fig. 2. The variations in the total energies as a function of the unit cell volumes of X2GdIn (X=Au, Ag or Cu).

Table 1
Lattice constant a (Å), bulk modulus B (in GPa), pressure derivative of bulk modulus B', elastic constants C_{ij} (in GPa), for Cu_2GdIn, Ag_2GdIn and Au_2GdIn compounds.

Compound		(GGA-WC)	GGA+U	LSDA	LSDA+U	Expt
Cu_2GdIn	a	6.70	6.587	6.50	6.498	6.447 [29] 6.641 [30] 6.6643 [31]
	B	82.60	95.234	109.32	106.209	–
	B'	4.47	5.029	5.52	4.692	–
Co_2CrBi [33]	B	132.7	–	–	–	–
	B'	5.20	–	–	–	–
Pd_2ZrAl [34]	B	151	–	–	–	–
Pd_2ZrIn [34]	B	141	–	–	–	–
Pd_2HfAl [34]	B	159	–	–	–	–
Pd_2HfIn [34]	B	150	–	–	–	–
	C_{11}	109.099	148.51	149.050	156.48	–
	C_{12}	70.011	85.42	86.944	84.20	–
	C_{44}	45.143	81.78	61.045	53.43	–
Ag_2GdIn	a	7.06	6.903	6.84	6.834	6.965 [28]
	B	81.27	86.435	96.66	97.088	–
	B'	5.52	5.513	5.16	5.407	–
	C_{11}	80.721	106.43	133.169	93.30	–
	C_{12}	65.816	98.35	81.903	103.51	–
	C_{44}	67.322	59.32	42.116	38.30	–
Au_2GdIn	a	7.06	6.938	6.86	6.857	6.94 [32]
	B	83.65	89.563	112.80	111.558	–
	B'	5.45	6.062	6.33	5.607	–
	C_{11}	89.301	125.39	119.770	107.32	–
	C_{12}	85.257	103.47	108.289	116.63	–
	C_{44}	57.101	51.70	50.572	45.91	–
Ni_2MnAl[37–40]	C_{44}	102[a], 64[b]	–	114.9[c],7.3[d]	–	–

[a] Ref. [37], PP/PAW_GGA-PW91.
[b] Ref. [38], FLAPW_GGA-PBE.
[c] Ref. [39], EMTO_LSDA.
[d] Ref. [40], FP-LMTO_LSDA.

Table 2
Shear modulus G, Young's modulus E (in GPa), Poisson's ration ν and Lamé's coefficients μ, λ and B/G (in GPa) for Cu_2GdIn, Ag_2GdIn and Au_2GdIn compounds.

Compound		(GGA-WC)	GGA+U	LSDA	LSDA+U
Cu_2GdIn	G	34.903	61.686	49.048	46.514
	E	91.782	152.197	128.001	121.766
	ν	0.315	0.234	0.305	0.309
	μ	34.903	61.686	49.048	46.514
	λ	8.139	15.355	11.672	10.982
	A	28.239	2.592	8.809	1.478
	B/G	2.366	1.883	2.228	2.283
Ag_2GdIn	G	43.374	37.208	35.523	20.938
	E	110.469	97.617	94.938	58.601
	ν	0.273	0.312	0.336	0.399
	μ	43.374	37.208	35.523	20.938
	λ	10.748	8.734	7.822	3.365
	A	9.033	14.683	1.643	–
	B/G	1.873	2.323	2.721	4.637
Au_2GdIn	G	33.069	35.404	32.639	25.684
	E	87.657	93.846	89.305	71.560
	ν	0.325	0.324	0.368	0.393
	μ	33.069	35.404	32.639	25.684
	λ	7.516	8.047	6.341	4.317
	A	2.309	4.717	1.965	4.343
	B/G	2.529	2.529	3.456	–
Ni_2MnAl [37–40]	G	32[a], 10[b]	–	15.6[c], 18.8[d]	–

[a] Ref. [37], PP/PAW_GGA-PW91.
[b] Ref. [38], FLAPW_GGA-PBE.
[c] Ref. [39], EMTO_LSDA.
[d] Ref. [40], FP-LMTO_LSDA.

effective parameter $U_{eff}=U-J$, where U is the Hubbard parameter and J is the exchange parameter. We set $U=7.07$ eV and $J=0.0$ eV. These parameters were sufficient to give good structural and elastic moduli.

3. Results and discussion

We have calculated the total energy as a function of the lattice constant for X_2GdIn in the ferromagnetic (FM) state. The plots of the calculated total energies versus the reduced volume of these compounds are given in Fig. 2. The total energies versus the changed volumes are fitted to Murnaghan's equation of state [27] to determine the ground state properties, such as the equilibrium lattice constant a, the bulk modulus B and its pressure derivative B'. The calculated structural parameters of these compounds are reported in Table 1. Our results for the lattice parameters are in good agreement with the experimental data [28–32]. Based on the experimental data, the equilibrium lattice constants for Ag_2GdIn and Au_2GdIn are best described by GGA+U, and Cu_2GdIn

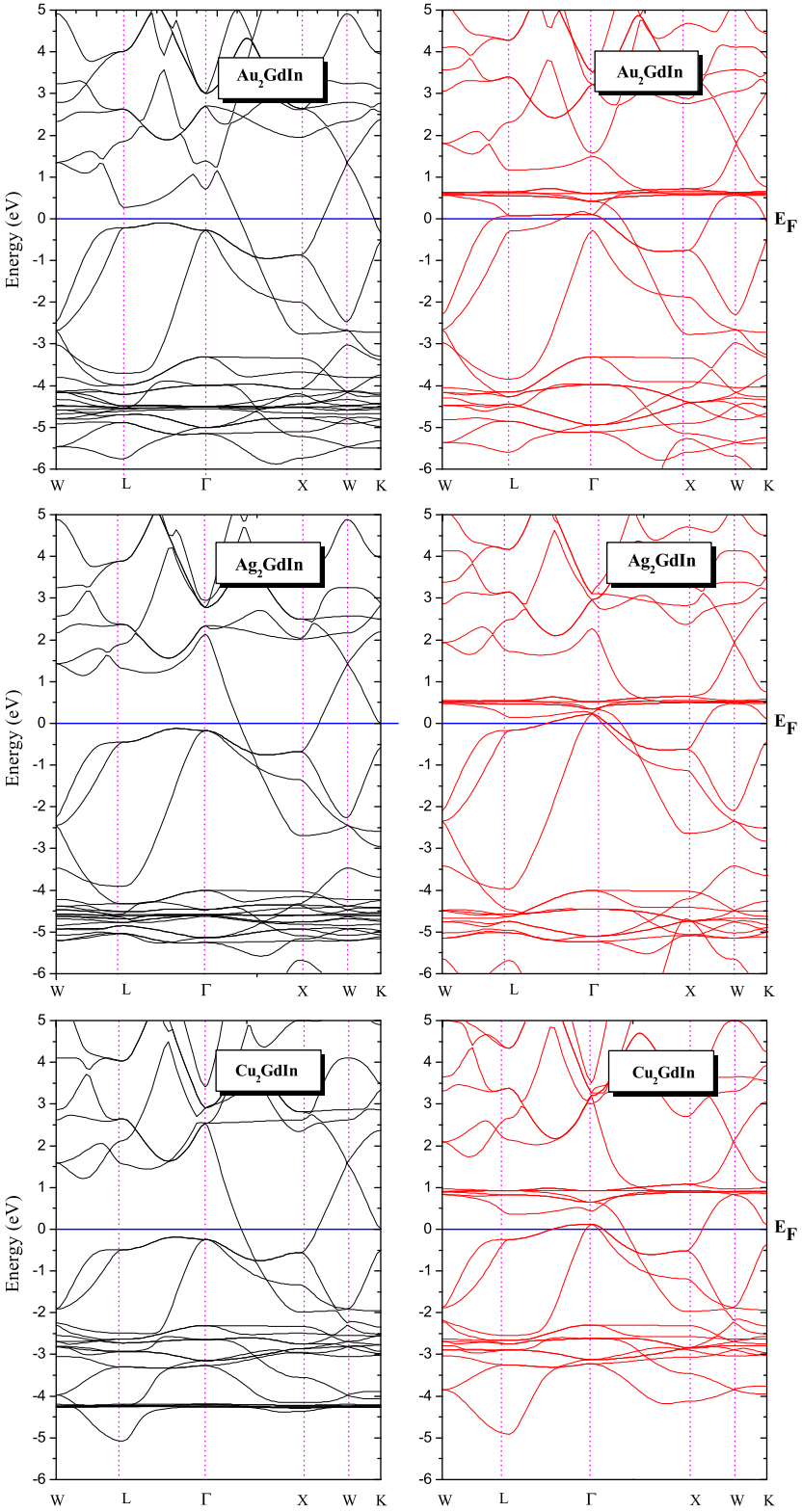

Fig. 3. The up- and down-spin band structures for X_2GdIn (X=Au, Ag or Cu) along the high-symmetry axes of the Brillouin Zone using GGA-WC.

is best described by LSDA+U, compared to the calculations by the GGA-WC and LSDA methods. To our knowledge, there are no previous experimental studies or theoretical calculations exploring the bulk modulus and its pressure derivative for these compounds. We also included the bulk modulus data for Co_2CrBi [33] and Pd_2ZrAl, Pd_2ZrIn, Pd_2HfAl and Pd_2HfIn [34] in Table 1 for comparison.

The elastic constants C_{ij} are the proportionality coefficients relating the applied strain to the stress, $\sigma_i = C_{ij}\varepsilon_i$. Hence, to study the stabilities of these compounds, we have calculated the elastic constants with the FP-LAPW method. A cubic crystal has only three independent elastic constants: C_{11}, C_{12} and C_{44}. Hence, a set of three equations is needed to determine all of constants. The first equation involves calculating the elastic constants C_{11} and C_{12}, which are related to the bulk modulus B.

$$B = \frac{1}{3}(C_{11}+2C_{12}). \tag{1}$$

The second one involves applying volume-conserving tetragonal strains:

$$\bar{\varepsilon} = \begin{pmatrix} \varepsilon & 0 & 0 \\ 0 & \varepsilon & 0 \\ 0 & 0 & \frac{1}{1+\varepsilon}-1 \end{pmatrix}. \tag{2}$$

The application of this strain changes the total energy from its initial value as follows:

$$E(\gamma) = (C_{11}-C_{12})6V_0\gamma^2 + 0(\gamma^3), \tag{3}$$

where V_0 is the volume of the unit cell. For the last type of deformation, we used the volume-conserving rhombohedral strain tensor that is given by

$$\bar{\varepsilon} = \begin{pmatrix} 1 & \frac{\varepsilon}{2} & 0 \\ \frac{\varepsilon}{2} & 1 & 0 \\ 0 & 0 & \frac{4}{(4-\varepsilon^2)} \end{pmatrix}, \tag{04}$$

which transforms the total energy to the full elastic tensor.

$$E(\gamma) = \frac{V_0}{3}(C_{11}+2C_{12}+4C_{44}) + 0(\gamma^3) \tag{05}$$

The individual elastic constants C_{ij} cannot be measured. Instead, the isotropic bulk modulus B and the shear modulus G are determined. For this purpose, we have utilized the Voigt-Reuss-Hill approximations. With this approach, the actual effective modulus for polycrystals can be approximated from the arithmetic mean of the two well-known bounds for monocrystals according to Voigt and Reuss. The Hill approximation is then used to determine the average [35] and is given by

$$G = (C_{11}-C_{12}+3C_{44})/5. \tag{06}$$

The Young's modulus E (which expresses the resistance of a material to unidirectional strain), Poisson's ratio v and the Lame coefficients (μ and λ) are frequently measured for polycrystalline materials to characterize their hardness.

These quantities are related to the elastic constants by the following equations:

$$E = 9\beta\cdot G/(3\beta+G) \tag{7}$$

$$v = (3\beta-E)/(6\beta) \tag{8}$$

$$\mu = E/(2(1+v)) \tag{9}$$

$$\lambda = vE/((1+v)(1-2v)) \tag{10}$$

The calculated elastic constants (C_{11}, C_{12} and C_{44}), the shear modulus G, Young's modulus E, Poisson's ratio v and Lamé's coefficients (μ and λ) are given in Tables 1 and 2.

The value of Poisson's ratio is small (v=0.1) for covalent materials, whereas 0.25 is a typical value of v for ionic materials [36]. A value of $\approx$0.3 for v indicates that the compound is an ionic material. To our knowledge, there are no previous experimental studies or theoretical calculations exploring the elastic constants, the shear modulus G, Young's modulus E, Poisson's ratio v and Lamé's coefficients (μ and λ). Thus, no experimental data for the elastic constants of these compounds are available. We included the shear modulus G and the C_{44} data of Ni_2MnAl [37–40] in the Tables 1 and 2 for comparison.

The requirement of mechanical stability in this cubic structure leads to the following restrictions on the elastic constants [41]:

$$C_{11}-C_{12} > 0, C_{44} > 0, C_{11}+2C_{12} > 0. \tag{11}$$

The Heusler compounds investigated here are based on cubic structures. Our results satisfy all of the criteria in Eq. (11), and it follows that these materials are stable in rocksalt (B1) structures. Au_2GdIn and Ag_2GdIn were obtained by the LSDA+U method.

We have calculated the anisotropy factor A (Table 2) of the compounds using the following expression for cubic symmetry:

$$A = 2*C_{44}/(C_{11}-C_{12}). \tag{12}$$

For an isotropic crystal, A is equal to 1, while any value smaller or larger than 1 indicates anisotropy.

A simple relationship that empirically links the plastic properties of materials with their elastic moduli was proposed by Pugh [42]. The shear modulus G represents the resistance to plastic deformation, while B represents the resistance to fracture [43].

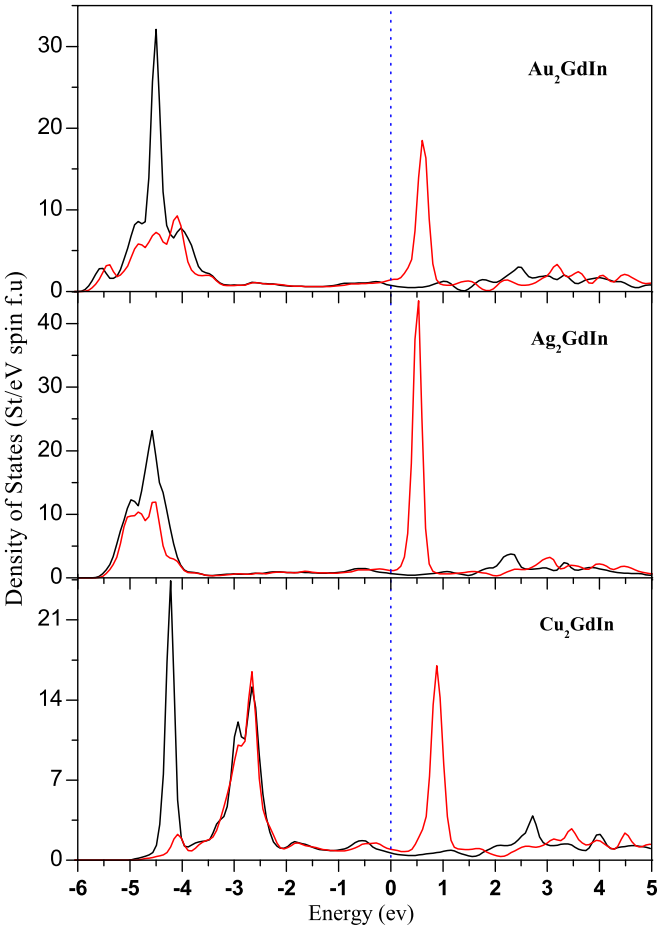

Fig. 4. The total density of states (TDOS) of Cu_2GdIn, Ag_2GdIn and Au_2GdIn using GGA-WC.

A high B/G ratio is associated with ductility, whereas a low value corresponds to a brittle nature. The critical value that separates ductile and brittle materials is approximately 1.75. If $B/G > 1.75$, then the material behaves in a ductile manner; otherwise the material behaves in a brittle manner. The calculated B/G for the X_2GdIn (X=Au, Ag or Cu) compounds are summarized in Table 2. These materials are classified as ductile.

The calculated spin-polarized band structures of the X_2GdIn (X=Au, Ag or Cu) compounds at the theoretical equilibrium lattice constant along the high-symmetry directions of the first

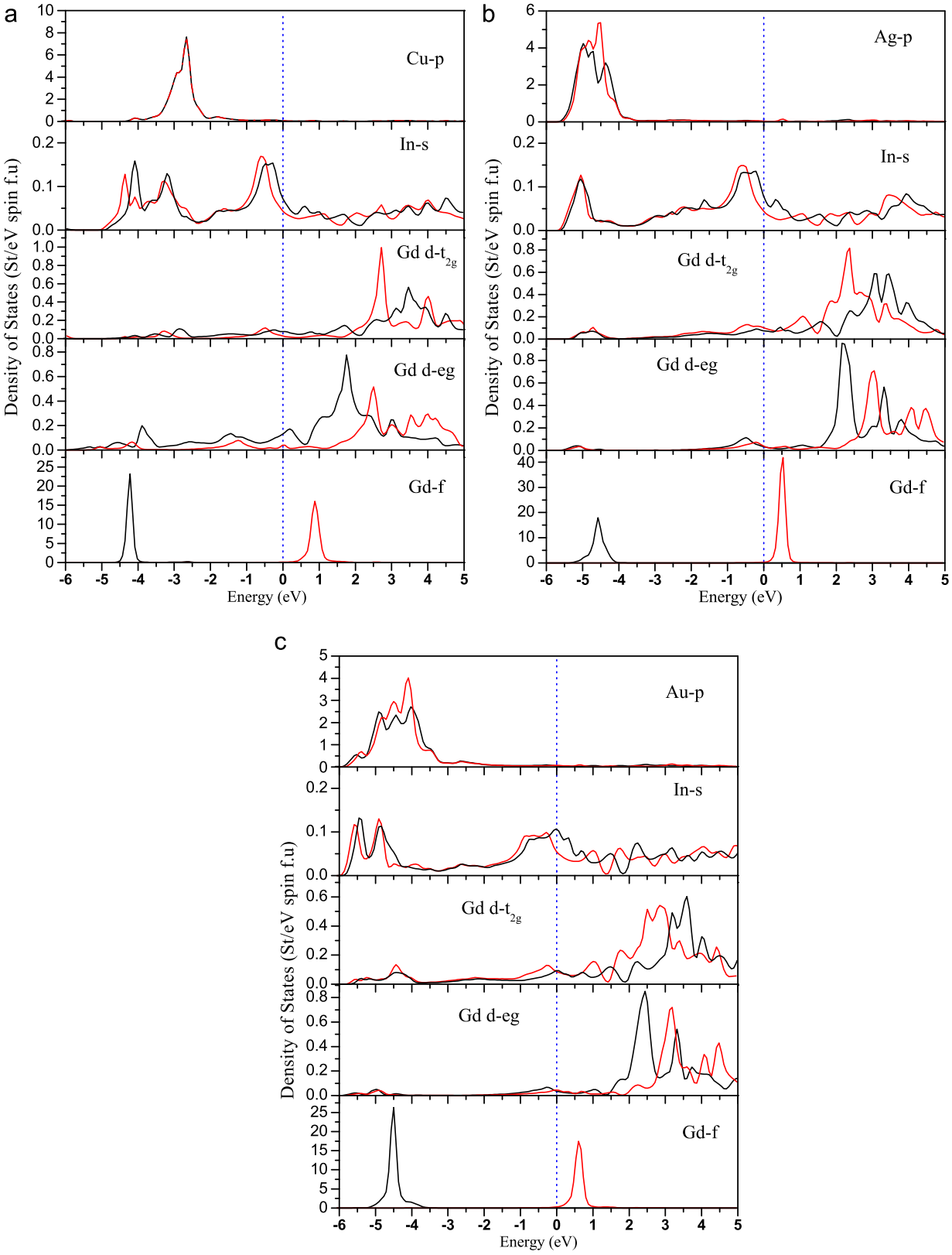

Fig. 5. The spin-polarized partial DOS of a) Cu2GdIn, b) Ag2GdIn and c) Au2GdIn using GGA-WC.

Table 3
Calculated total and partial magnetic moment (in μ_B) for X_2GdIn (X=Au, Ag and Cu) compounds.

Compound		Interstitial region	Gd	In	X	Total magnetic moment	Expt
Cu_2GdIn	(GGA-WC)	0.11850	6.98155	−0.01252	−0.00316	7.08120	7.89 [30]
	GGA+U	0.09736	6.67904	−0.01114	0.01018	6.86233	7.98 [32]
	LSDA	0.09301	6.95811	−0.00968	0.01078	7.06300	–
	LSDA+U	0.08283	6.78784	−0.00458	0.01230	6.89071	–
Ag_2GdIn	(GGA-WC)	0.13266	6.97955	−0.01562	−0.00310	7.09040	–
	GGA+U	0.09886	6.75455	−0.00557	−0.00027	6.84730	–
	LSDA	0.10822	6.95877	−0.01234	0.00304	7.06073	–
	LSDA+U	0.09963	6.73672	−0.00442	0.00139	6.83470	–
Au_2GdIn	(GGA-WC)	0.16020	6.96555	−0.00538	0.00052	7.12142	–
	GGA+U	0.11580	6.77229	−0.00272	0.00114	6.88765	–
	LSDA	0.12219	6.93454	−0.00434	0.00697	7.06634	–
	LSDA+U	0.08211	6.73515	−0.00519	0.00401	6.82009	–

Brillouin zone are displayed in Fig. 3. The total and partial densities of states, in which the spin-up and spin-down sub-bands are plotted with black and red lines, respectively, are shown in Figs. 3–5. The Fermi level was set to 0 eV.

In Fig. 3, the non-existence of a gap at the Fermi level for both compounds confirms the metallic behavior and indicates the presence of conducting features.

In Fig. 4 shows the total density of states (TDOS) as a function of energy for the lattice constant of X_2GdIn (X=Au, Ag or Cu). To illustrate the nature of the electronic band structures, we have plotted the partial density of states (DOS) of X-p, In-s, Gd (eg and t_{2g}) and Gd-4f for the spin-up and spin-down sub-bands in Fig. 5. For all of the cases, the figure indicates that band structures can be divided into three parts: (1) −6.0 eV to 0.0 eV, which represents the contribution of the majority spin of the 4f orbital of Gd atoms hybridized with X p states and In s electrons, (2) 0.0 to 1.5 eV, where the 4f orbital of Gd atoms creates fully unoccupied bands (the exchange-splitting between the spin-up and spin-down sub-bands of the Gd 4f states is approximately 5.0 eV, which is the main contributor in the magnetic moment of these compound) and (3) 1.5 to 5.0 eV, where strong Gd (eg and t_{2g}) states exist in the majority and minority spin states.

The calculated total and atom-resolved magnetic moments, using different approximations (GGA-WC, GGA+U, LSDA and LSDA+U), are summarized in Table 3. The present study shows that the total magnetic moment for all three compounds is $\approx 7.08\mu_B$ for the GGA-WC approximation. Here, the values of the total magnetic moment vary from 6.82 to 7.07. When we used the U-Hubbard term, the magnetic moment decreased significantly. For Cu_2GdIn, the total magnetic moment agrees with recent experimental data [30,32]. For these Heusler compounds, the magnetic moments originate from the exchange-splitting of the 4f states of the rare-earth ions. Our results for the magnetic moment of the Gd atom (Table 3) shows agreement between the experimental data of $7.94\mu_B$ [32] and the theoretical value $\mu_{eff}^{th} = g\mu_B\sqrt{j(j+1)}$ of $7.94\mu_B$ [44]. For the X_2GdIn compounds, most of the magnetic moment arises from Gd atoms, as expected, because gold, silver, copper and indium atoms carry no magnetic moment.

4. Conclusions

Here, using the FP-LAPW methods implemented in Wien2k (GGA-WC, GGA+U, LSDA and LSDA+U), the structural, electronic, elastic and magnetic properties of Cu_2GdIn, Ag_2GdIn and Au_2GdIn Heusler compounds were investigated. The electronic structures of the ferromagnetic configurations for X_2GdIn Heusler compounds are metallic in character. The calculated lattice constants are in good agreement with the experimental data. A numerical first-principles method was used to calculate the elastic constants C_{ij}, the shear modulus G, Young's modulus E, Poisson's ration v and Lamé's coefficients (μ and λ). The values of the B/G ratios for the X_2GdIn compounds show that these materials are ductile. The magnetic moment contributions were primarily from the rare-earth Gd 4f ion. Our calculations show that Heusler compounds (X_2GdIn) are promising materials in future spintronic applications.

References

[1] P.J. Webster, K.R.A. Ziebeck, Magnetic Alloy and Compounds of d-Elements with Main Group Elements (Landolt-Börnstein New Series Group III, vol 19c), in: H.P.J. Wijn (Ed.), Springer, Berlin, 1988, p. 75. K. R. A. Ziebeck and K-U. Neuman Magnetic Properties of Metals (Landolt-Börnstein New Series Group III,vol 32) ed H P J Wijn (Berlin: Springer) p 64 (2001).
[2] S.A. Wolf, D.D. Awschalom, R.A. Buhrman, J.M. Daughton, S. von Molnar, M.L. Roukes, A.Y. Chtchelkanova, D.M. Treger, Science 294 (2001) 1488.
[3] G.A. Prinz, Science 282 (1998) 1660.
[4] Y. Ohno, D.K. Young, B. Beshoten, F. Matsukura, H. Ohno, D.D. Awschalom, Nature 402 (1999) 790.
[5] T. Dietl, H. Ohno, F. Matsukura, J. Cibert, D. Ferrand, Science 287 (2000) 1019.
[6] J.H. Park, E. Voscovo, H.J. Kim, C. Kwon, R. Ramesh, T. Venkatesh, Nature 392 (1998) 794.
[7] R.A. de Groot, F.M. Mueller, P.G.v Engen, K.H.J. Buschow, Phys. Rev. Lett. 50 (1983) 2024.
[8] M. Ishikawa, J.L. Jorda, A. Junod, Superconductivity in d- and f-band metals 1982, W. Buckel and W. Weber, Kernforschungszentrum Karlsruhe, Germany, 1982.
[9] J.H. Wernick, G.W. Hull, J.E. Bernardini, J.V. Waszczak, Mater. Lett. 2 (1983) 90.
[10] H.A. Kierstead, B.D. Dunlap, S.K. Malik, A.M. Umarji, G.K. Shenoy, Phys. Rev. B 32 (1985) 135.
[11] R.N. Shelton, L.S. Hausermann-Berg, M.J. Johnson, P. Klavins, H.D. Yang, Phys. Rev. B 34 (1986) 199.
[12] H.C. Kandpal, G.H. Fecher, C. Felser, J. Phys. D: Appl. Phys. 40 (2007) 1507.
[13] C. Felser, G.H. Fecher, B. Balke, Angew. Chem. Int. Ed. 46 (2007) 668.
[14] T. Marukame, T. Ishikawa, S. Hakamata, K. Matsuda, T. Uemura, M. Yamamoto, Appl. Phys. Lett. 90 (2007) 012508.
[15] N. Tezuka, N. Ikeda, S. Sugimoto, K. Inomata, Appl. Phys. Lett. 89 (2006) 252508.
[16] A.D. Bianchi, E. Felder, A. Schilling, M.A. Chernikov, F. Hulliger, H.R. Ott, Z. Phys. B 99 (1995) 69.
[17] D.B. de Mooij, K.H.J. Buschow, J. Less-Comm. Met. 102 (1984) 113.
[18] P. Hohenberg, W. Kohn, Phys. Rev. B 136 (1964) 864.
[19] W. Kohn, L.J. Sham, Phys. Rev. A 140 (1965) 1133.
[20] J.C. Slater, Adv. Quant. Chem. 1 (1964) 5564.
[21] P. Blaha, K. Schwarz, G.K.H. Madsen, D. Kvasnicka, J. Luitz, WIEN2K, an Augmented Plane Wave +Local orbitals program for calculating crystal properties, Karlheinz Schwarz, Technische Universität, Wien, Austria, ISBN 3-9501031-1-2, 2001.
[22] Z. Wu, R.E. Cohen, Phys. Rev. B 73 (2006) 235116.
[23] J.P. Perdew, W. Wang, Phys. Rev. B 45 (13) (1992) 244;
P. Blaha, K. Schwarz, P. Sorantin, S.B. Tricky, Chem. Phys. Lett. (1990) 399.
[24] C. Loschen, J. Carrasco, K.M. Neyman, F. Illas, Phys. Rev. B 75 (2007) 035115.
[25] V.I. Anisimov, J. Zaanen, O.K. Andersen, Phys. Rev. B 44 (1991) 943;
V.I. Anisimov, I.V. Solovyev, M.A. Korotin, M.T. Czyzyk, G.A. Sawatzky, Phys. Rev. B 48 (1993) 16929.
[26] H.J. Monkhorst, J.D. Pack, Phys. Rev. B 13 (1976) 5188.
[27] F.D. Murnaghan, Proc. Natl. Acad. Sci. USA 30 (1944) 244.

[28] R.M. Galera, J. Pierre, E. Siaud, A.P. Murani, J. Less-Common Met. 97 (1984) 151.
[29] I. Felner, Solid State Commun. 56 (1985) 315.
[30] K.-U. Neumann, J. Crangle, D. Visser, N.K. Zayer, K.R.A. Ziebeck, Phys. Lett. A 177 (1993) 99.
[31] Z.M. Pu Wang, J. Stadnik, Phys.: Condens Matter 19 (2007) 346235.
[32] M.J. Besnus, J.P. Kappler, M.F. Ravet, A. Meyer, R. Lahiouel, J. Pierre, E. Siaud, G. Nieva, J. Sereni, Journal of the Less-Common Metals 120 (1986) 101.
[33] G. Ökhan, G. Ökoğlu, Physica B 405 (2010) 2162–2165.
[34] J. Winterlik, G.H. Fecher, A. Thomas, C. Felser Phys. Rev. B (2009)064508.
[35] J.F. Nye, Propriétés physiques des matériaux, Dunod, 1961.
[36] J. Haines, J.M. Leger, G. Bocquillon, Ann. Rev. Mater. Res. 31 (2001) 1.
[37] H.B. Luo, C.M. Li, Q.M. Hu, R. Yang, B. Johansson, L. Vitos, Acta Materialia 59 (2011) 971–980.
[38] H. Rached, D. Rached, R. Khenata, A.H. Reshak, M. Rabah, Phys Status Solidi B 246 (2009) 1580.
[39] T. Busgen, J. Feydt, R. Hassdorf, S. Thienhaus, M. Moske, M. Boese, et al., Phys Rev B 70 (2004) 014111.
[40] A. Ayuela, J. Enkovaara, K. Ullakko, R.M. Nieminen, J.: Phys. Condens Matter 11 (1999) 2017.
[41] B. Holm, R. Ahuja, Y. Yourdshahyan, B. Johanson, B.I. Lundqvist, Phys. Rev. 59 (1999) 12777.
[42] S.F. Pugh, Philos. Mag 45 (1954) 823.
[43] G. Vaitheeswaran, V. Kanchana, R.S. Kumar, A.L. Cornelius, M.F. Nicol, A. Savane, A. Delin, B. Johansson, Phys. Rev. B 76 (2007) 014107.
[44] S. Blundell, Magnetism in Condensed Matter, Oxford University Press, Oxford, 2001.